17th World Conference on Earthquake Engineering, 17WCEE
Sendai, Japan - September 13th to 18th 2020

INTELLIGENT SYSTEM FOR ACCELEROGRAPHIC PROCESSING IN PERU

J. Alva [1], C. Ortiz [2], M. Chipana [2], J. Valverde [2]

[1] *Principal Researcher, National University of Engineering, jalvah@uni.edu.pe*
[2] *Researcher, National University of Engineering, cortiz@uni.edu.pe, mchipanai@uni.pe, jvalverdea@uni.edu.pe*

Abstract

Peru is located in a high seismic hazard zone as its territory is subject to the interaction of the Nazca and South American Plates, as well as surface faulting which also generate large earthquakes along the continent. These seismic events create seismic forces that impact structures, frequently causing numerous material and human losses to vulnerable buildings throughout Peruvian territory.

The last major seismic events to have occurred in Peru were in 2001, in Arequipa, and in 2007, in Pisco, reaching magnitudes Mw 8.4 and 7.9, respectively. When these earthquakes took place, Peru did not have enough instrumentation to measure seismic events so they were only recorded by few stations. This lack of information led the National Engineering University (UNI) in 2014, through the Faculty of Civil Engineering' Accelerographic Network, to acquire the necessary instruments to implement eighty accelerograph stations which are now installed in different cities of our country.

An Intelligent System for Accelerographic Processing, known as SIPA, (for its acronym in Spanish) was also developed additionally to this instrumentation. This system uses intelligent algorithms (neural networks) that help process accelerograms such a degree that reports are created automatically and in real time. Such data includes history time records, response spectra and Fourier spectra, spectral ratio. This benefits researches greatly as they now have more time to focus on correctly interpreting the information obtained, thus allowing them to contribute to improving seismic risk management in our country.

SIPA is an information system capable of determining whether or not an accelerogram contains a seismic event. To perform this task, neural networks are used. This paper will describe the topology of the neural network, as well as the performance tests obtained during in recent years. Training and evaluation of the neural network used 2016 to 2018 accelerograms, and the backpropagation method was used for the training.

The paper also includes as an example the Mw 8 Lagunas earthquake report, dated May 26, 2019 at 2:41 a.m., which occurred in Lagunas, Alto Amazonas, Loreto, in the northeastern part of Peru. The Accelerographic Network's Intelligent System for Accelerographic Processing (SIPA) recorded the event at 44 different accelerographic stations, the highest recorded acceleration being 95.84 gal, which allowed to learn about the amplification and attenuation of the accelerations, as well as the dynamic behavior of the soil of the different cities in which this equipment was installed.

Keywords: neural networks; accelerographic network; intelligent system

1. Introduction

Peru is located in a high seismic hazard zone, in which the most recent major seismic events of 8.4 Mw=8.4 and Mw=7.9 occurred in 2001, in Arequipa, and in 2007, in Pisco, respectively. At the time, Peru did not have sufficient instrumentation to measure seismic events, so few stations were able record such events. This led to the National Engineering University (UPG FIC-UNI) in 2014, through the Faculty of Civil Engineering' Accelerographic Network, to acquire the necessary instruments to implement eighty accelerographic stations. These have now been installed in different cities throughout the country so as to contribute to and supplement the information currently being provided by other accelerometric networks, This will generate greater knowledge of the dynamic behavior of soils ultimately allowing us to come up with recommendations and develop regulations for structure design and construction for earthquake-resistant buildings.

Additionally, our country still works with accelerographic networks that do not have automated processing and reporting, requiring people to work a greater number of hours. To help with these tasks, the Intelligent System for Accelerographic Processing was created which now uses artificial intelligence to process such information. This was achieved in a two-stage design process: development of the event-detection algorithm, and the development of an intelligent system which takes the processing algorithm into consideration. These are described below.

2. Development of Classification Algorithm

2.1 Data

The classification algorithm was developed using accelerometric records taken between 2017 and 2018 for neural network training and validation purposes. Such data include 2,277 records containing seismic events and 10,179 records without seismic events. Each record contains 3 channels so there is a signal for each axis (North-South, East-West and Vertical).

The neural network takes as input a single signal, that means that for each record the network must return a 3-results vector which each result corresponds each channel signal.

2.2 Pre-processing

We developed a neural network that receives as input the information in the frequency domain because we consider that changes are more visible in that domain and also earthquakes in Peru have greater amplitude between the 0.1 to 25 Hz frequencies. In order to perform a visual inspection, the spectrogram was plotted as is shown in Fig. 1, where the spectrogram is shown between the periods of 0.1 to 25 Hz.

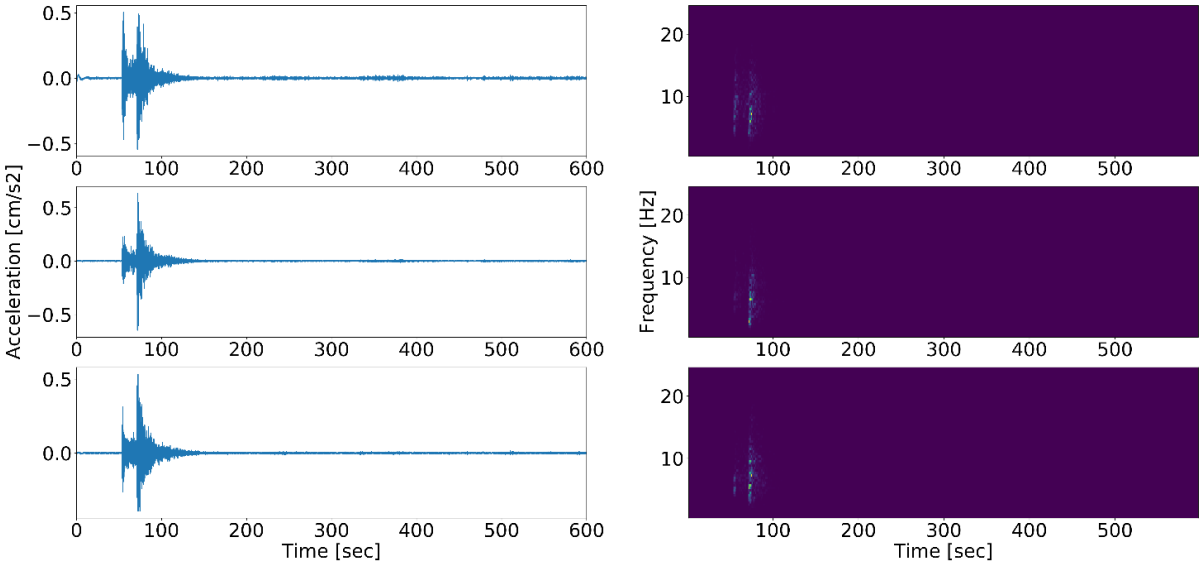

Fig. 1 – Acceleration and spectrogram of a seismic event record

2.3 Data Augmentation

The proportion ‘with earthquake’ and ‘without earthquake’ files was approximately 1:5, so in order to balance this out, the data for seismic events was increased. For this reason, we developed a function to cut the spectrogram to 80 and 60 percent of its initial length, in addition to displacing 60 and 120 samples. The result was that for each spectrogram we were able to obtain 4 additional spectrograms. The neural network thus can receive input data of different time lengths and the pattern in different positions as shown in Fig. 2 where the transformations made to the spectrograms are shown.

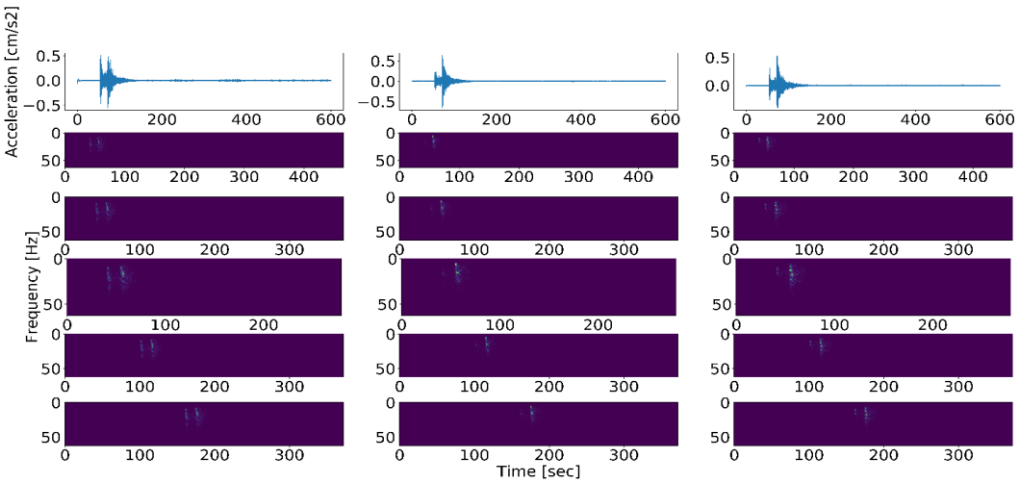

Fig. 2 – Results of the data increase function

On the other hand, the spectrograms of the records without seismic events were cut into random lengths, which resulted in 34,155 seismic event spectrograms and 30,537 without seismic event. Finally, each spectrogram was resized to a 60 x 180 matrix.

2.4 Neural Network Architecture

This paper considered a convolutional neural network architecture [1] because, according to the authors, it is one of the most used models in the field of deep learning [1] and with which very good results have been obtained in different applications.

Table 1 summarizes the architecture used, where the layer column describes the type of layer, the shape column the shape of the output matrix, and the parameters column the number of trainable parameters for each layer. The network is made up of three sets of convolutional layers, where each set consists of a Convolutional Layer followed by a Max Pooling Layer [2] and a Dropout Layer. Those initial layers are in charge of reducing the initial matrix to a matrix with the most important features, later a fully-connected neural network of two layers of 512 and 2 neurons each is used which is responsible for classifying the features already identified.

Table 1 – Neural Network Architecture

LAYER	SHAPE	PARAMETERS
Conv2d_1	(58, 178, 32)	320
Max_pooling2d_1	(29, 89, 32)	0
Dropout_1	(29, 89, 32)	0
Conv2d_2	(27, 87, 32)	9248
Max_pooling2d_2	(13, 43, 32)	0
Dropout_2	(13, 43, 32)	0
Conv2d_3	(11, 41, 16)	4624
Max_pooling2d_3	(5, 20, 16)	0
Dropout_3	(5, 20, 16)	0
Flatten	(1600)	0
Dense_1	(512)	819712
Dense_2	(2)	1026
TOTAL		834930

2.5 Training and Validation

70% of the data was used for training purposes, using the backpropagation method [2], Cross Entropy function [1] was used as a Loss Function because it is recommended for classification applications. Also, we tested different optimizers but found that Adam optimizer [3] had the best performance, obtaining an accuracy of 99.56%. Fig. 3 shows a graph of the training accuracy evolution. The remaining 30% of data was used for validation purposes. During validation, 98.77% accuracy was obtained.

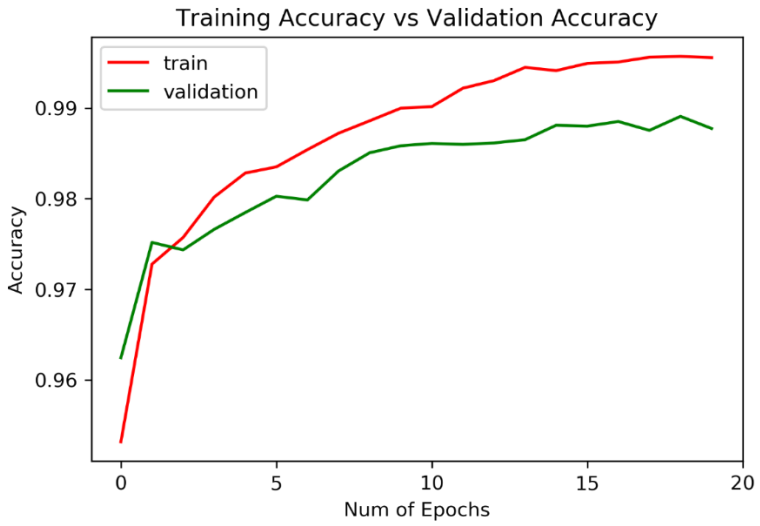

Fig. 3 – Training Accuracy vs Validation Accuracy

In order to better appreciate the performance, the confusion matrix is shown in Fig. 4 and other parameters such as accuracy, recall [3] and the F1-Score were calculated in Table 2. As can be seen, the accuracy of 'event' class is 99.20%, a good result as the goal of our application is that it detects the events, and even though 'recall' [3] is a little lower, we concluded that the developed network fulfills its purpose.

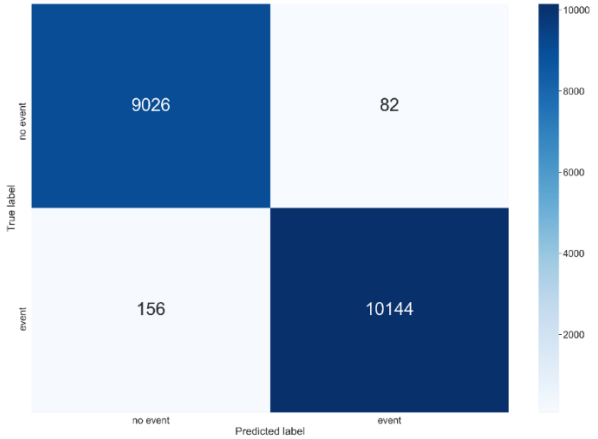

Fig. 4 – Confusion matrix

Table 2 – Other parameters

CLASSIFICATION	PRECISION	RECALL	F1-SCORE
NO EVENT	0.9830	0.9910	0.9870
EVENT	0.9920	0.9849	0.9884

2.6 Evaluation

Two data sets were used to evaluate the neural network. The first consisted of 2016 records, a total of 2,214 (299 of which were events), and the second data set consisted of 124 important earthquake records of varying duration and different sampling rates. Each set of data obtained accuracy results of 97.75% and 98.87%, respectively

2.7 Flowchart

Fig. 5 depicts the classification algorithm process. First, the accelerometric record input is received and is used to calculate the spectrogram from 0 to 25 Hz for each channel. Next, the matrix is resized to 60 x 180 and this resulting matrix is then used as input for the neural network. Finally, the results of each channel are grouped into a single vector which is the algorithm's output.

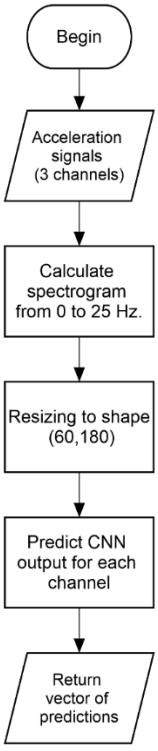

Fig. 5 – Flowchart of the classification algorithm

3. Description of the Intelligent System

The explanation above corresponds to an algorithm capable of classifying accelerometric records. The process is illustrated by the system flowchart (Fig. 6). REFTEK software is used to obtained the accelerometric files required to begin the process. These are then classified by the convolutional neural network described above. Based on the result of the neural network, the algorithm determines which files will be sent to the processing algorithm and which will be removed from the process. All process results are saved in a database. After processing the files, a report the Intelligent System produces a report which is published on the FIC-UNI Accelerographic Network website. (Fig. 7)

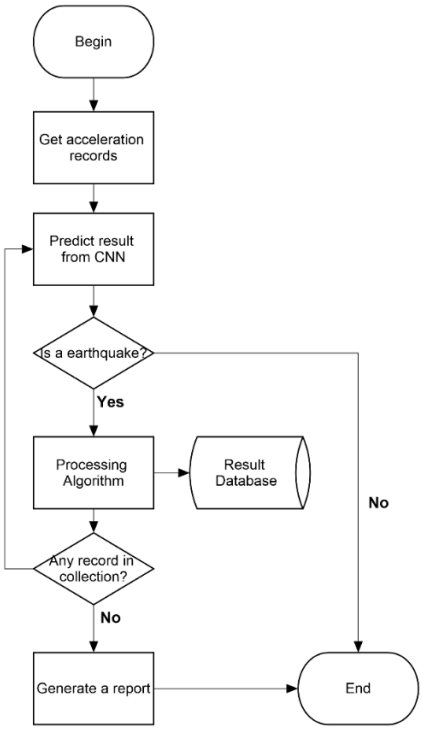

Fig. 6 – System flowchart

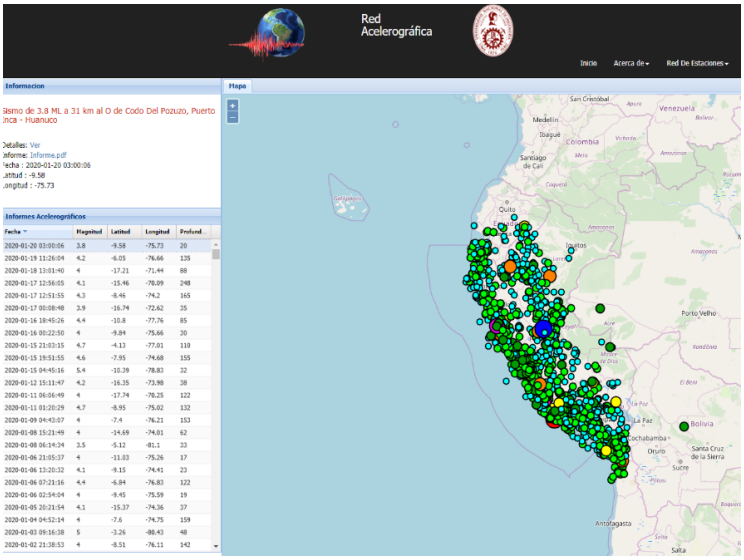

Fig. 7 – System website. www.red-acelerografica-peru.com

3.1 Processing Algorithm

Fig. 8 illustrates the steps involved in algorithm processing. First, baseline correction is used to compensate the record data which is then filtered to a 0.1 to 25 Hz range (corresponding to the frequencies observed over the years in Peru). Following this, the Fourier spectrum is calculated, followed by the Response spectrum, and, finally seismic parameters are calculated and the final results are delivered.

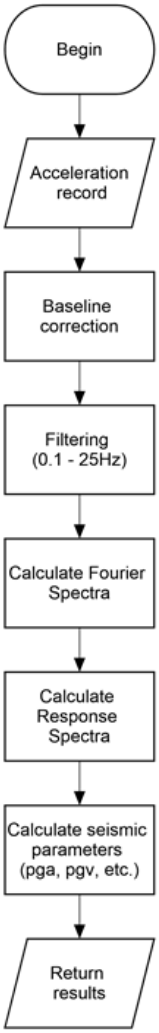

Fig. 8 – Diagram of the processing algorithm

With regard to baseline correction, an arithmetic mean of the data was used, for which each point of the original signal is subtracted from the arithmetic mean of the data as presented in equations Eq. (1), Eq. (2) and Eq. (3).

Original signal:

$$X = [x_1\ x_2\ x_3\ \dots\ x_{n-2}\ x_{n-1}\ x_n] \tag{1}$$

Mean:

$$\mu = \frac{1}{n}\sum_{i=1}^{n} x_i \tag{2}$$

Corrected data: The arithmetic mean is subtracted at each point of the signal.

$$Y = X - \mu \tag{3}$$

Moreover, the Butterworth filter is applied to the signal because, compared to other filters, it does not present curling in the band of interest (0.1 Hz to 25 Hz) (Fig. 9). This filter has an order of up to 4 because raising the order could cause instability in the resulting system, making it would be necessary to divide the system (Eq. (4)) into second-order subsystems (Eq. (5)). [4]

Transfer Function of a Butterworth filter of order 4:

$$H(z) = \frac{Y(z)}{X(z)} = \frac{b_0 + b_1 z^{-1} + b_2 z^{-2} + b_3 z^{-3} + b^4 z^{-4}}{1 + a_1 z^{-1} + a_2 z^{-2} + a_3 z^{-3} + a^4 z^{-4}} \quad (4)$$

Transfer function based on its poles and zeros, and separation into two subsystems:

$$H(z) = k\left(\frac{(z-c_1)(z-c_2)}{(z-p_1)(z-p_2)}\right)\left(\frac{(z-c_3)(z-c_4)}{(z-p_3)(z-p_4)}\right) \quad (5)$$

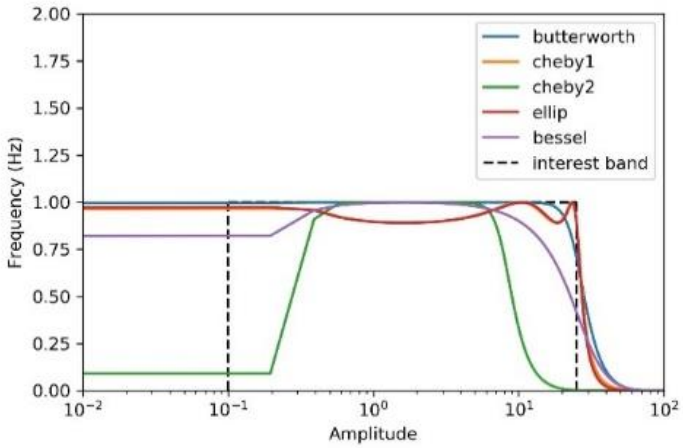

Fig. 9 – Comparison of different filters in the band of interest

The Fourier amplitude spectrum is calculated using the Fast Fourier Transform (FFT), which is an algorithm used to quickly calculate the Discrete Fourier Transform (Eq. (6)) of the time series record. The Fourier amplitude spectrum shows how the amplitude of soil movement is distributed with respect to the frequency or period. [6].

$$X(m) = \sum_{n=0}^{N-1} x(n) e^{-j\frac{2\pi n m}{N}} \quad (6)$$

The response spectrum is calculated using the eight constants method [5] which is based on the solution of Duhamel's Integral and its equations Eq. 7 and Eq. 8, for N periods equalized between a Tmin and a Tmax.

$$u_{i+1} = Au_i + B\dot{u}_i + Cp_i + Dp_{i+1} \quad (7)$$

$$\dot{u}_{i+1} = A'u_i + B'\dot{u}_i + C'p_i + D'p_{i+1} \quad (8)$$

4. Results of the Intelligent System for Accelerographic Processing (SIPA)

SIPA's results, 1,745 accelerographic reports for the years 2017-2019, were prepared and published on the website. Table 3 and Table 4 show the statistics of the reports based on magnitudes and accelerations, respectively.

Table 3 – Number of accelerographic reports in relation to the magnitudes

Range of Magnitude	N° of Reports	N° Accelerometers	
		min	max
ML <= 5	1619	1	26
5 < Mw <= 7	123	1	34
Mw>7	3	28	44

Table 4 – Number of accelerographic reports in relation to accelerations.

Range of Accelerations (cm/s^2)	N° of Reports
<10	1595
<10, 50]	135
<50, 100]	10
<100, 400]	5

One of the results obtained using SIPA, was the report for the magnitude Mw = 8 Lagunas earthquake which took place in Lagunas, Alto Amazonas, Loreto, in the northeastern part of Peru on May 26, 2019 at 2:41 am. The earthquake occurred as the result of normal faulting at an intermediate depth of 110 km [6]. The earthquake resulted in 4,562 casualties, 40 rural roads were destroyed [7], as were 131 homes, and a further 1,270 homes were left uninhabitable. Some of the damage can be seen in Fig. 10.

Fig. 10 – Land damage in the populated center January 6 [8], in the district of Santa Cruz (Left), Loreto - Peru and destroyed housing [9] in the district of Sauce (right), San Martín - Peru.

The Accelerographic Network's Intelligent System for Accelerographic Processing (SIPA) recorded the event at 44 different stations (Fig. 11). The highest recorded acceleration was 95.84 cm / s2. Table 5 provides data taken from the 4 stations with the highest records, including accelerations, the Arias intensity (Iα) and the specific energy density (SED). Additionally, for comparative purposes, the information obtained at the Lima CIP station on rigid ground is included.

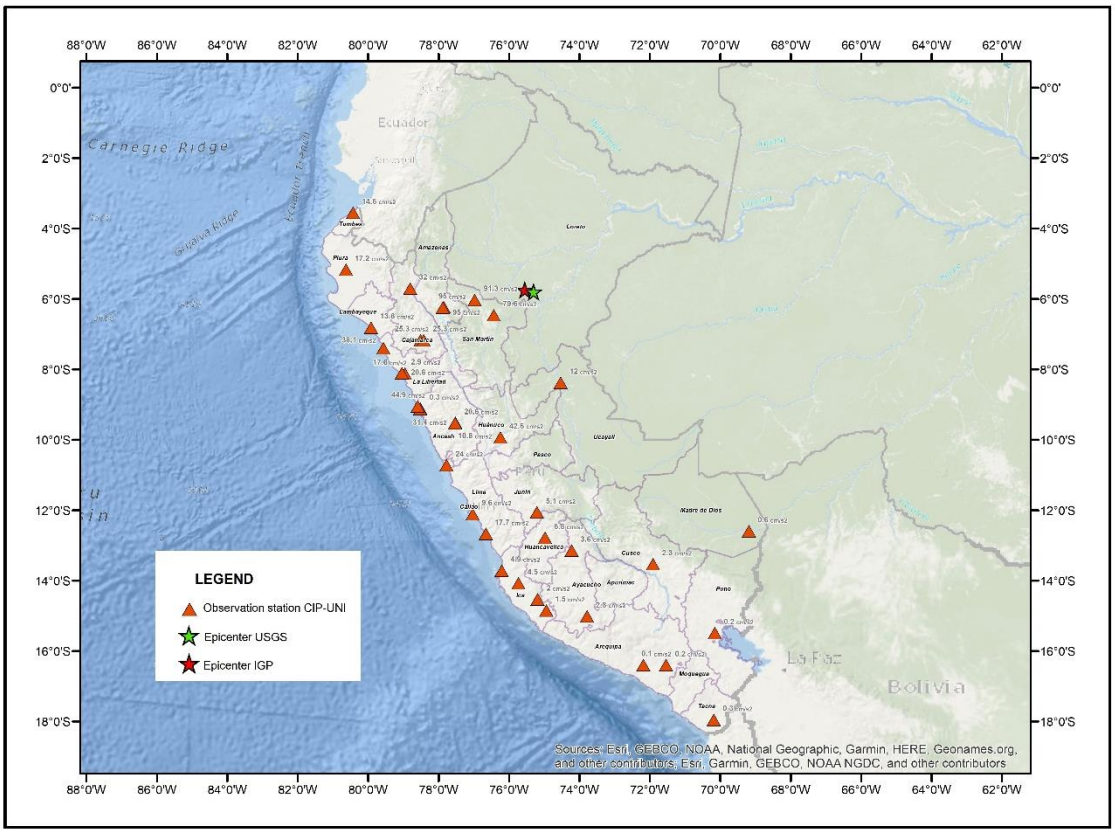

Fig. 11 – Stations that recorded the Lagunas earthquake of May 26, 2019

Table 5 – Stations with the highest records of the Lagunas Earthquake and the CIP Lima record

Earthquake	Station	Comp.	PGA cm/s^2	PGV cm/s	PGD, cm	V_{max} /A_{max}, sec	RMS Acc, g	RMS Vel, cm/s	RMS Disp, cm	I_a m/s	SED, m^2/s
Lagunas-Alto Amazonas, Loreto, Peru 2019	UNTRM	EO	95.84	13.46	2.62	0.14	11.06	1.32	0.29	0.87	772.04
		NS	87.45	8.34	1.49	0.10	10.64	1.06	0.20	0.81	501.81
		V	53.49	3.52	0.92	0.07	6.64	0.44	0.12	0.31	84.23
	CIP MOYOBAMBA	EO	91.29	19.13	6.62	0.21	12.96	3.40	1.51	0.81	3469.17
		NS	78.76	20.85	9.14	0.26	12.39	3.48	1.64	0.74	3623.72
		V	90.16	13.08	4.21	0.15	11.43	2.09	0.70	0.63	1312.25
	CIP TARAPOTO	EO	58.18	9.00	3.04	0.15	14.15	2.03	1.07	0.35	451.00
		NS	79.56	10.70	3.34	0.13	16.19	2.13	0.79	0.46	491.97
		V	67.86	4.74	1.26	0.07	10.56	1.03	0.38	0.19	115.30
	CIP AMAZONAS	EO	78.91	7.32	1.70	0.09	7.79	0.79	0.20	0.43	275.13
		NS	53.98	5.84	1.11	0.11	7.16	0.75	0.17	0.36	249.44
		V	53.05	3.07	0.93	0.06	5.26	0.41	0.13	0.20	75.30
	CIP LIMA	EO	11.06	0.74	0.28	0.07	0.92	0.08	0.06	0.01	2.89
		NS	10.43	0.54	0.26	0.05	0.88	0.07	0.04	0.01	2.11
		V	6.78	0.37	0.17	0.05	0.68	0.05	0.04	0.00	1.25

SIPA also generated a report [10] which shows the accelerations, velocities, displacements, Fourier Spectra and Response Spectra for each station. Records were obtained from all regions of Peru, an aspect that allowed to know and compare the dynamic behavior of the different types of soil. Fig. 12, for example, shows the Response spectrum for a soft soil of the clayey type recorded by the UNTRM station at an epicentral distance of 292 km and a maximum acceleration of 95.84 cm/s2, while Fig. 13 shows the Response Spectrum for a rigid gravelly soil recorded by the CIP Lima station at an epicentral distance of 733 km and a maximum acceleration of 11.06 cm/s2.

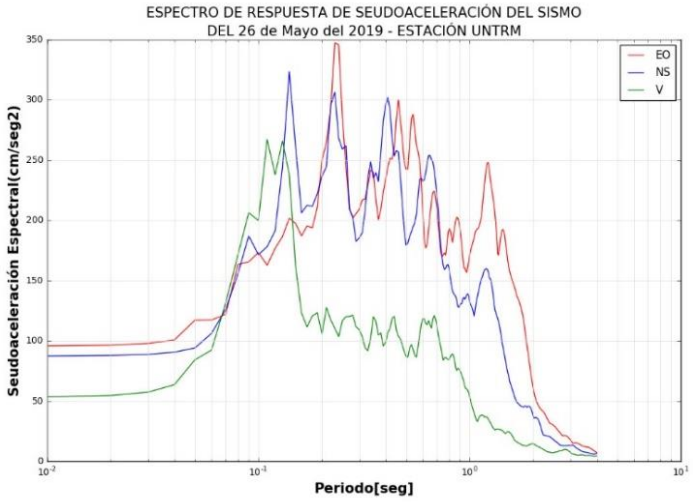

Fig. 12 – Response spectrum of the UNTRM Station, which corresponds to a soft ground

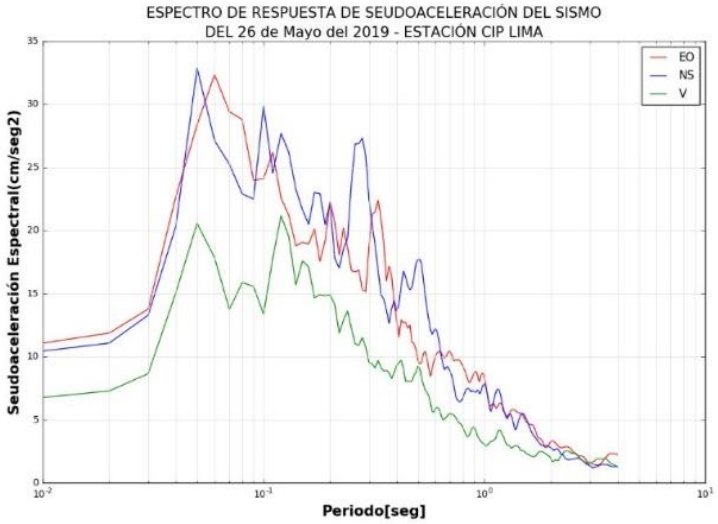

Fig. 13 – Response spectrum of the LIMA CIP Station, which corresponds to a rigid ground

5. Conclusions

The automation of accelerographic record processing, through SIPA, improved FIC UNI Accelerographic Network's performance, reducing the reporting times to a maximum of thirty minutes after the seismic event occurred.

The use of neural networks proved to be effective in the detection of seismic events, obtaining accuracies of approximately 98%, improving their performance the more data they use for its training.

The report generated by SIPA for the Lagunas earthquake which took place on May 26, 2019 contributed to the information used by our country's institutes – in charge of the Seismic Risk Management – for immediate response in the aftermath of these types of events.

The information reported by SIPA allowed for the development of Iso-acceleration maps, and to prepare recommendations to update the structure design and construction regulations for earthquake-resistant buildings in Peru.

6. Acknowledgements

Thanks to the National University of Engineering for their support in preparing this paper.

7. References

[1] Trask A (2019): *Grokking Deep Learning*. Manning Publications Co, 1st edition.

[2] Russell S, Norving P (2003): *Artificial Intelligence: A Modern Approach*. Pearson, 2nd edition.

[3] Goodfellow et al (2016): *Deep Learning*. MIT Press, 1st edition

[4] Lyons GR (2011): *Understanding Digital Signal Processing*, 3rd Edition.

[5] Chopra AK (2014): *Dynamics of Structures*, 4th Edition, 167-171.

[6] U.S. Geological Survey, Earthquake M 8.0 - 78km SE of Lagunas, Peru, available online at https://earthquake.usgs.gov/earthquakes/eventpage/us60003sc0/executive

[7] INDECI(2019): *Emergency report N° 850 - 27/12/2019 / COEN - INDECI / 12:00* (in Spanish) Informe de Emergencia N° 850 - 27/12/2019 / COEN - INDECI / 12:00 Horas

[8] Newspaper 'El Comercio', Picture: Alonso Chero.

[9] Newspaper 'Perú 21', Picture: Rolly Reyna.

[10] CIP-UNI Accelerographic Network (2019): *Final Report Lagunas earthquake, Alto Amazona, Loreto on May 26 2019* (in Spanish) Informe Final Red Acelerográfica CIP – UNI Sismo Lagunas - Alto Amazonas - Loreto 26 de Mayo de 2019.

